The MCPM, a two-Higgs-doublet model with maximal CP symmetry, and LHC13

M. Maniatis[1,*] and O. Nachtmann[2,†]

[1] *Departamento de Ciencias Básicas, UBB, Casilla 447, Chillán, Chile.*
[2] *Institut für Theoretische Physik, Philosophenweg 16, 69120 Heidelberg, Germany*

We continue our investigation of the phenomenological consequences of the MCPM for the LHC experiments. As in any two-Higgs-doublet model we have in the MCPM three neutral Higgs bosons and one charged Higgs-boson pair $H^\pm$. Here we discuss the two-photon production in proton-proton collisions. We find that in the MCPM a resonance-type structure in the $\gamma\gamma$ invariant mass distribution is predicted around twice the $H^\pm$ mass $m_{H^\pm}$ with a width $2\,\Gamma_H$ where Γ_H is the $H^\pm$ width. If we set $m_{H^\pm} = 375$ GeV, the above resonance structure appears at 750 GeV with a width of about 45 GeV. We point out various predictions of the MCPM which follow in such a scenario and which can be checked at the LHC.

arXiv:1606.01231v1 [hep-ph] 3 Jun 2016

1. INTRODUCTION

One of the aims of the present LHC experiments is the exploration of the scalar sector of particle physics. Indeed, one scalar particle was already found in brilliant experiments [1, 2]. But it is not clear if Nature corresponds to the Standard Model (SM) where we have only one physical Higgs boson. Many models with extended scalar sectors exist in the literature. An attractive alternative to the SM are two-Higgs-doublet models, THDMs; see [3, 4] and references therein. In our group we emphasised the usefulness of bilinears for the study of THDMs [5–9]. A THDM with maximal CP symmetry has been presented in [9]. This model, the *maximal CP symmetric model*, MCPM, gives a certain understanding of family replication and fermion mass hierarchies. Phenomenological consequences of the MCPM were worked out in [10–14]. In the present paper we continue the phenomenological investigations of the MCPM in view of the possibilities of the experiments at LHC13. We shall, in particular, be interested in two-photon production in proton-proton collisions.

Our paper is organised as follows. In section 2 we briefly review some features of the MCPM. In section 3 we present the details of the calculation of diphoton production in proton-proton collisions. Section 4 contains our discussion and section 5 our conclusions.

2. BRIEF REVIEW OF THE MCPM

In this section we recall briefly some main features of the MCPM. Like in any two-Higgs-doublet model there are five physical Higgs bosons, in our notation, ρ', $H^\pm$, h'', h'. The ρ' behaves on its mass shell very similarly to the SM Higgs boson which we denote by $\rho'_{\rm SM}$. Thus, we set for the mass of the ρ' the measured value from [1, 2].

$$m_{\rho'} = 125 \text{ GeV}. \tag{2.1}$$

The masses of the charged Higgs-boson pair, $H^\pm$, of the pseudoscalar h'' and of the scalar h' are not predicted by the model except that the hierarchy

$$m_{h''} < m_{h'} \tag{2.2}$$

is required. The model is built to have the generalised CP symmetry of type (i), see [9], and this has drastic consequences. The couplings of the Higgs bosons among themselves are determined in terms of the masses. Furthermore, in the strict symmetry limit and concerning the Yukawa couplings, the third fermion family couples exclusively to the ρ', the second family only to $H^\pm$, h'', h', but with coupling constants related to the third family. The first family of fermions is uncoupled to the Higgs sector in this limit where the masses of the second and first-family fermions are zero. Of course, this is not realistic, but it is not so bad as a first approximation to Nature; see [9]. In the following we will work in this strict symmetry limit. Thus, all relations are subject to corrections from symmetry breaking.

*E-mail: maniatis8@gmail.com
†E-mail: O.Nachtmann@thphys.uni-heidelberg.de

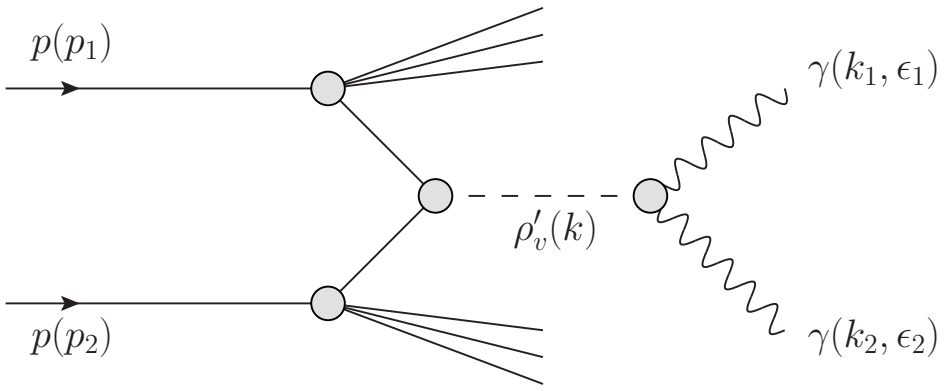

FIG. 1: Diphoton production in proton-proton collision via an intermediate virtual Higgs boson ρ'_v.

But in this paper we are interested in the physics of the Higgs bosons of the MCPM, that is, physics at the 100 to 800 GeV scale. We expect that symmetry breaking corrections due to the non-zero masses of the first and second fermion family will be small in this regime. The Lagrangian of the MCPM is given explicitly in appendix A of [10].

3. THE MCPM AND THE REACTION $pp \to \gamma\gamma X$

In the following we shall study the reaction of two protons, $p(p_1)$ and $p(p_2)$, giving a pair of photons, $\gamma(k_1, \epsilon_1)$ and $\gamma(k_2, \epsilon_2)$, via an intermediate virtual Higgs boson $\rho'_v(k)$, and a rest X, see Fig. 1,

$$p(p_1) + p(p_2) \to \rho'_v(k) + X \to \gamma(k_1, \epsilon_1) + \gamma(k_2, \epsilon_2) + X. \tag{3.1}$$

Here the momentum and polarization vectors are indicated in brackets. The **T**-matrix element for this process is

$$i\langle\gamma(k_1, \epsilon_1), \gamma(k_2, \epsilon_2), X|\mathbf{T}|p(p_1), p(p_2)\rangle = \\ i\langle\gamma(k_1, \epsilon_1), \gamma(k_2, \epsilon_2)|\mathbf{T}|\rho'_v(k)\rangle \frac{i}{k^2 - m^2_{\rho'} + im_{\rho'}\Gamma_{\rho'}} i\langle\rho'_v(k), X|\mathbf{T}|p(p_1), p(p_2)\rangle, \tag{3.2}$$

with $k = k_1 + k_2$, and $m_{\rho'}$, $\Gamma_{\rho'}$ the mass and width of the Higgs boson ρ', respectively. The invariant mass squared of the photon pair and the square of the center-of-mass collision energy are defined as usual,

$$m^2_{\gamma\gamma} = (k_1 + k_2)^2, \qquad s = (p_1 + p_2)^2. \tag{3.3}$$

For unpolarized protons as well as unobserved polarizations of the photons we find the cross section

$$\frac{d\sigma}{dm^2_{\gamma\gamma}}(p(p_1) + p(p_2) \to \gamma(k_1) + \gamma(k_2) + X(p_X)) = \\ \frac{1}{2\sqrt{s(s - 4m_p^2)}} \frac{1}{2} \int \frac{d^4k_1}{(2\pi)^3} \delta_+(k_1^2) \int \frac{d^4k_2}{(2\pi)^3} \delta_+(k_2^2) \\ \times \sum_X (2\pi)^4 \delta^{(4)}(k_1 + k_2 + p_X - p_1 - p_2)\ \delta_+((k_1 + k_2)^2 - m^2_{\gamma\gamma}) \\ \times \sum_{\text{spins}} \left|\langle\gamma(k_1, \epsilon_1), \gamma(k_2, \epsilon_2)|\mathbf{T}|\rho'_v(k)\rangle\right|^2 \left|m^2_{\gamma\gamma} - m^2_{\rho'} + im_{\rho'}\Gamma_{\rho'}\right|^{-2} \\ \times \frac{1}{4} \sum_{\text{spins}} \left|\langle\rho'_v(k), X(p_X)|\mathbf{T}|p(p_1), p(p_2)\rangle\right|^2. \tag{3.4}$$

Now we define the production cross section for the virtual Higgs boson ρ'_v

$$\sigma(p(p_1)+p(p_2)\to\rho'_v(m^2_{\gamma\gamma})+X)=\frac{1}{2\sqrt{s(s-4m_p^2)}}\sum_X\int\frac{d^4k}{(2\pi)^3}\delta_+(k^2-m^2_{\gamma\gamma})$$
$$\times(2\pi)^4\delta^{(4)}(k+p_X-p_1-p_2)\,\frac{1}{4}\sum_{\text{spins}}\left|\langle\rho'_v(k),X(p_X)|\mathbf{T}|p(p_1),p(p_2)\rangle\right|^2. \quad (3.5)$$

We define the decay width of the virtual boson ρ'_v of mass squared $m^2_{\gamma\gamma}$ as

$$\Gamma(\rho'_v(m^2_{\gamma\gamma})\to\gamma\gamma)=\frac{1}{2m_{\gamma\gamma}}\frac{1}{2}\int\frac{d^4k_1}{(2\pi)^3}\delta_+(k_1^2)\int\frac{d^4k_2}{(2\pi)^3}\delta_+(k_2^2)$$
$$\times(2\pi)^4\delta^{(4)}(k_1+k_2-k)\sum_{\text{spins}}\left|\langle\gamma(k_1,\epsilon_1),\gamma(k_2,\epsilon_2)|\mathbf{T}|\rho'_v(k)\rangle\right|^2. \quad (3.6)$$

With this we have for the cross sections

$$\frac{d\sigma}{dm^2_{\gamma\gamma}}(p(p_1)+p(p_2)\to\gamma(k_1)+\gamma(k_2)+X)=$$
$$\sigma(p(p_1)+p(p_2)\to\rho'_v(m^2_{\gamma\gamma})+X)\frac{m_{\gamma\gamma}}{\pi}\left|m^2_{\gamma\gamma}-m^2_{\rho'}+im_{\rho'}\Gamma_{\rho'}\right|^{-2}\Gamma(\rho'_v(m^2_{\gamma\gamma})\to\gamma\gamma) \quad (3.7)$$

and

$$\frac{d\sigma}{dm_{\gamma\gamma}}(p(p_1)+p(p_2)\to\gamma(k_1)+\gamma(k_2)+X)=$$
$$\sigma(p(p_1)+p(p_2)\to\rho'_v(m^2_{\gamma\gamma})+X)\frac{2m^2_{\gamma\gamma}}{\pi}\left|m^2_{\gamma\gamma}-m^2_{\rho'}+im_{\rho'}\Gamma_{\rho'}\right|^{-2}\Gamma(\rho'_v(m^2_{\gamma\gamma})\to\gamma\gamma). \quad (3.8)$$

3.1. Production of ρ'_v

The couplings of the Higgs boson ρ' to the gauge bosons and fermions of the third generation are like those for the SM Higgs boson ρ'_{SM}. For the production reaction

$$p(p_1)+p(p_2)\to\rho'_v(k)+X \quad (3.9)$$

we have, therefore, the following main processes:

- gluon-gluon fusion,

$$G+G\to\rho'_v, \quad (3.10)$$

- vector-boson fusion,

$$W^+ + W^-\to\rho'_v,\qquad Z+Z\to\rho'_v, \quad (3.11)$$

- fusion of $t\bar{t}$ and $b\bar{b}$ quarks,

$$t+\bar{t}\to\rho'_v,\qquad b+\bar{b}\to\rho'_v. \quad (3.12)$$

Therefore, the production cross section (3.5) can be calculated as for a SM Higgs boson ρ'_{SM} of mass $m_{\gamma\gamma}$ but we have to leave out very small contributions to ρ'_{SM} production from the annihilation of first and second generation quark-antiquark pairs. All this has already been discussed in [10, 11] and we can thus rely on the results presented there for the cross section (3.5).

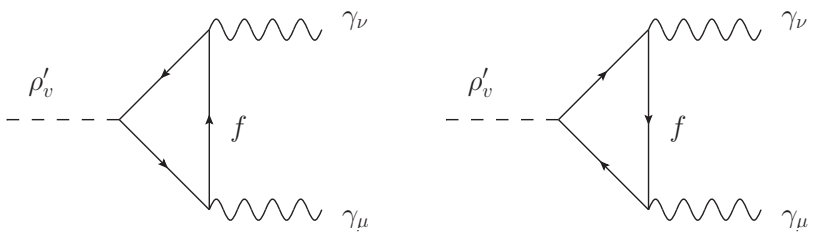

FIG. 2: Fermion loop contributions to $\rho_v' \to \gamma\gamma$ for $f = t,\, b,\, \tau$.

3.2. The decay $\rho_v' \to \gamma\gamma$

For the decay of the virtual Higgs boson ρ_v' to two photons we have in the MCPM contributions from fermion loops, $W^\pm$-boson loops, and $H^\pm$ loops. The latter contributions will be of particular interest for us in the following. From gauge invariance and Bose symmetry we can write the amplitude for

$$\rho_v'(k) \to \gamma(k_1, \epsilon_1) + \gamma(k_2, \epsilon_2) \tag{3.13}$$

as follows

$$\begin{aligned} &\langle \gamma(k_1,\epsilon_1), \gamma(k_2,\epsilon_2) | \mathbf{T} | \rho_v'(k) \rangle = e^2 \epsilon_1^{\mu *} \epsilon_2^{\nu *} T_{\mu\nu}(k_1, k_2), \\ &T_{\mu\nu}(k_1,k_2) = \big[-(k_1 k_2) g_{\mu\nu} + k_{2\mu} k_{1\nu} + k_{1\mu} k_{2\nu} \big] T(k^2). \end{aligned} \tag{3.14}$$

Here $T(k^2)$ is a scalar function receiving contributions from the above mentioned loops which we discuss now in turn.

- Fermion loops

  The ρ_v' couples to the third generation fermions t, b, τ like the SM Higgs boson ρ_{SM}'; see Fig. 2. The calculation of this contribution to $T(k^2)$ in (3.14) is standard (see e.g. [3, 10]) and gives, with the couplings as specified in appendix A of [10],

  $$T_f(k^2) = -\frac{1}{8\pi^2 v_0} 4 N_c^f e_f^2 \frac{m_f^2}{k^2} F_{1/2}^{\rho'} \left(\frac{4m_f^2}{k^2} \right), \qquad f = t, b, \tau. \tag{3.15}$$

  Here $v_0 = 246$ GeV is the standard Higgs vacuum-expectation value, e_f is the charge of the fermion f in units of the positron charge, and N_c^f is the colour factor,

  $$N_c^f = \begin{cases} 3, \text{ for } f = t, b, \\ 1, \text{ for } f = \tau. \end{cases} \tag{3.16}$$

  The function $F_{1/2}^{\rho'}(z)$ is given by

  $$F_{1/2}^{\rho'}(z) = -2\big[1 + (1-z) f(z)\big], \qquad f(z) = \begin{cases} -\frac{1}{4}\Big[\ln\left(\frac{1+\sqrt{1-z}}{1-\sqrt{1-z}} \right) - i\pi \Big]^2, \text{ for } 0 < z < 1, \\ \arcsin^2\left(\frac{1}{\sqrt{z}} \right), \text{ for } z \geq 1. \end{cases} \tag{3.17}$$

  For $\sqrt{z}$ and $\sqrt{1-z}$ in (3.17) the positive branches of the square roots have to be taken.

- $W^\pm$ loops

  The diagrams for this contribution are shown in Fig. 3. Also here the couplings of ρ_v' to $W^\pm$ are as those for ρ_{SM}' to $W^\pm$. Again, we can take over the standard expressions for this contribution to $T(k^2)$ in (3.14) (see [3, 10])

  $$T_W(k^2) = -\frac{1}{8\pi^2 v_0} F_1 \left(\frac{4m_W^2}{k^2} \right), \quad F_1(z) = 2 + 3z + 3z(2-z) f(z). \tag{3.18}$$

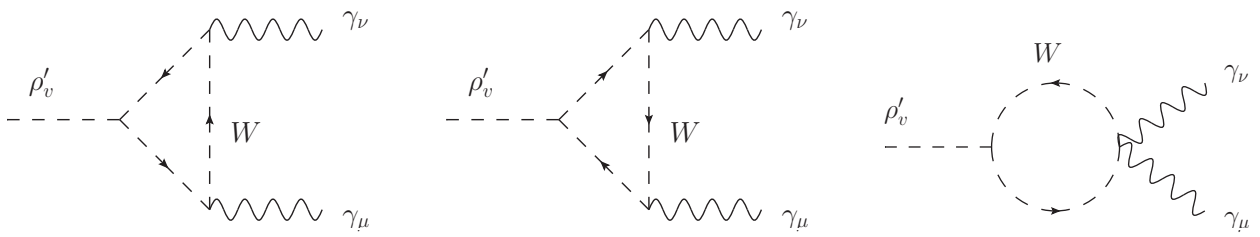

FIG. 3: $W^\pm$ loop contributions to $\rho'_v \to \gamma\gamma$.

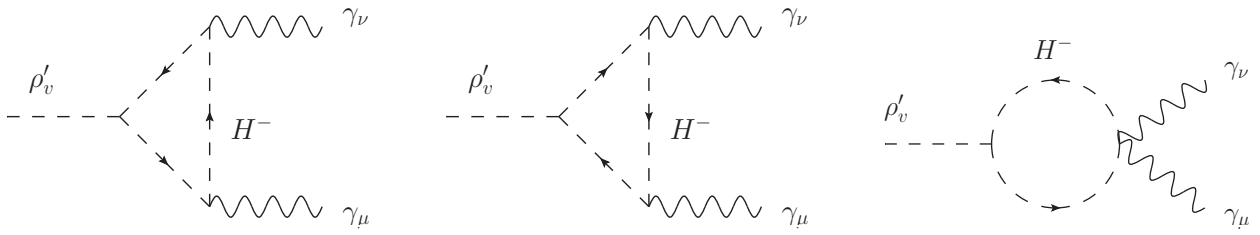

FIG. 4: $H^\pm$ loop contributions to $\rho'_v \to \gamma\gamma$.

- $H^\pm$ loops

  The diagrams for this contribution, which has no analogue in the SM, are shown in Fig. 4. Here we encounter the $\rho' H^+ H^-$ vertex which is given, in the MCPM, as follows (see appendix A of [10])

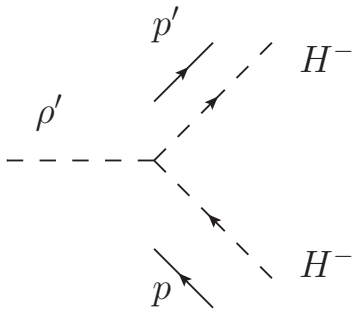

$$i\Gamma^{(\rho' HH)}(p', p) = -i\frac{m^2_{\rho'} + 2m^2_{H^\pm}}{v_0}.$$

  Now, everything is fixed and we get from the diagrams of Fig. 4 the result

$$T^{(2)}_{H^\pm} = -\frac{1}{8\pi^2 v_0}\frac{m^2_{\rho'} + 2m^2_{H^\pm}}{2m^2_{H^\pm}} F_0\left(\frac{4m^2_{H^\pm}}{k^2}\right), \quad \text{where } F_0(z) = z - z^2 f(z); \tag{3.19}$$

  see chapter 3.3 of [10].

But the result (3.19) is not the whole story. In the following we shall be mainly interested in the H^+H^- threshold region

$$k^2 = m^2_{\gamma\gamma} \approx 4m^2_{H^\pm}. \tag{3.20}$$

There, as we show now, we have large effects from H^+H^- interactions. Indeed, the exchange of ρ' and γ between H^+ and H^- near threshold leads to an attractive potential $V(\mathbf{x})$ between them, consisting of a Yukawa and a Coulomb term; see Fig. 5. We get

$$V(\mathbf{x}) = -\frac{\kappa}{r}e^{-m_{\rho' r}} - \frac{\alpha}{r}, \tag{3.21}$$

where

$$r = |\mathbf{x}|, \qquad \alpha = \frac{e^2}{4\pi}, \qquad \kappa = \frac{1}{4\pi}\frac{1}{4m^2_{H^\pm}}\left(\frac{m^2_{\rho'} + 2m^2_{H^\pm}}{v_0}\right)^2. \tag{3.22}$$

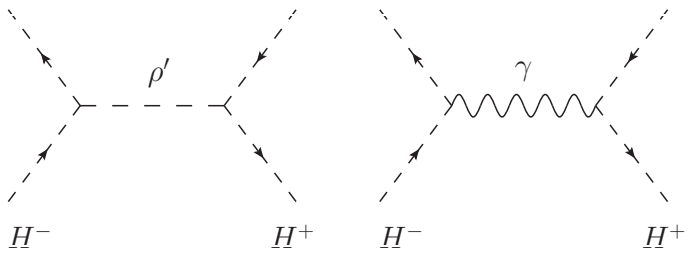

FIG. 5: Diagrams of ρ' and γ exchange between H^- and H^+ leading to the potential (3.21).

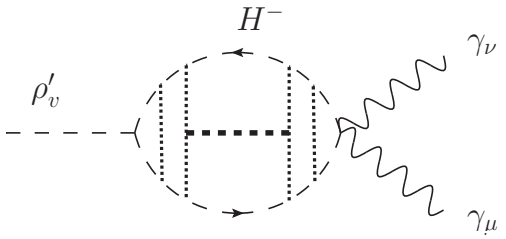

FIG. 6: Diagram of $\rho'_v \to \gamma\gamma$ in the threshold region (3.20). The dotted lines stand for the exchange due to the potential (3.21).

To calculate the effects of the potential (3.21) on $\rho'_v \to \gamma\gamma$ in the threshold region (3.20) we rely on the methods developed for $t\bar{t}$ production in its threshold region in [15–18]. It is easy to see that in the threshold region (3.20) the amplitude for the reaction $H^-H^+ \to \gamma\gamma$ is dominated by the $H^-H^+\gamma\gamma$ contact term. Therefore, for $\rho'_v \to \gamma\gamma$ in the threshold region we have to evaluate the diagram shown in Fig. 6. According to the methods of [15–18] we set

$$\sqrt{k^2} = 2m_{H^\pm} + E, \qquad |E| \ll 2m_{H^\pm} \tag{3.23}$$

and consider the following Green's function $G(\mathbf{x}, \mathbf{y}, E)$ defined by the equation

$$(\hat{H} - i\Gamma_H - E)G(\mathbf{x}, \mathbf{y}, E) = \delta^{(3)}(\mathbf{x} - \mathbf{y}). \tag{3.24}$$

Here Γ_H is the width of $H^\pm$ and $\hat{H}$ is the Hamilton operator

$$\hat{H} = -\frac{1}{m_{H^\pm}}\Delta_x + V(\mathbf{x}) \tag{3.25}$$

with $V(\mathbf{x})$ from (3.21) and Δ_x the Laplace operator. Suppose then, that the eigenvalue problem for $\hat{H}$ has been solved. We expect to find discrete eigenvalues

$$\hat{H}\Psi_{\alpha,\beta}(\mathbf{x}) = E_\alpha \Psi_{\alpha,\beta}(\mathbf{x}) \tag{3.26}$$

for $E_\alpha < 0$ labeled by $\alpha = 1, 2, \ldots$ and possibly a degeneracy index β. We normalise the eigenfunctions to

$$\int d^3x \Psi^*_{\alpha',\beta'}(\mathbf{x})\Psi_{\alpha,\beta}(\mathbf{x}) = \delta_{\alpha',\alpha}\delta_{\beta',\beta}. \tag{3.27}$$

For energies greater or equal to zero we will get a continuous spectrum

$$\hat{H}\Psi_\beta(\mathbf{x}, E') = E'\Psi_\beta(\mathbf{x}, E'), \qquad E' \geq 0. \tag{3.28}$$

Here, again, β is a possible degeneracy label and we normalise the eigenfunctions to

$$\int d^3x \Psi^*_{\beta'}(\mathbf{x}, E')\Psi_{\beta''}(\mathbf{x}, E'') = \delta_{\beta',\beta''}\delta(E' - E''). \tag{3.29}$$

We have then the completeness relation

$$\sum_{\alpha,\beta} \Psi_{\alpha,\beta}(\mathbf{x})\Psi^*_{\alpha,\beta}(\mathbf{y}) + \int_0^\infty dE' \sum_\beta \Psi_\beta(\mathbf{x}, E')\Psi^*_\beta(\mathbf{y}, E') = \delta^{(3)}(\mathbf{x} - \mathbf{y}). \tag{3.30}$$

The Green's function $G(\mathbf{x}, \mathbf{y}, E)$ is given by

$$G(\mathbf{x}, \mathbf{y}, E) = \sum_{\alpha,\beta} \Psi_{\alpha,\beta}(\mathbf{x}) \frac{1}{E_\alpha - E - i\Gamma_H} \Psi^*_{\alpha,\beta}(\mathbf{y}) + \int_0^\infty dE' \sum_\beta \Psi_\beta(\mathbf{x}, E') \frac{1}{E' - E - i\Gamma_H} \Psi^*_\beta(\mathbf{y}, E'). \tag{3.31}$$

Formally the amplitude corresponding to the diagram of Fig. 6 is given by

$$T_H^{(1)}(4m_{H^\pm}^2 + 4m_{H^\pm}E) = \frac{1}{4m_{H^\pm}^4} \frac{m_{\rho'}^2 + 2m_{H^\pm}^2}{v_0} G(0, 0, E), \tag{3.32}$$

a result which is, however, divergent if we extend the integration over E' in (3.31) up to infinity. But this is not justified since we have to restrict all energies to be in absolute value much small than $2m_{H^\pm}$, the threshold energy. Thus, we introduce a cutoff parameter E_0 with

$$0 < E_0 \ll 2m_{H^\pm} \tag{3.33}$$

and extend the integral in (3.31) only up to $E' = E_0$. We get then from (3.23) and (3.31) to (3.33)

$$T_H^{(1)}(k^2) = \frac{1}{m_{H^\pm}^3} \frac{m_{\rho'}^2 + 2m_{H^\pm}^2}{v_0} \Bigg\{ \sum_{\alpha,\text{S waves}} \frac{|\Psi_\alpha(0)|^2}{4m_{H^\pm}^2 + 4m_{H^\pm}E_\alpha - i4m_{H^\pm}\Gamma_H - k^2} + \int_{0,\text{S waves}}^{E_0} dE' \frac{|\Psi(0, E')|^2}{4m_{H^\pm}^2 + 4m_{H^\pm}E' - i4m_{H^\pm}\Gamma_H - k^2} \Bigg\}. \tag{3.34}$$

Note that only the S waves contribute here since we evaluate the Green's function for $\mathbf{x} = \mathbf{y} = 0$.

In order to obtain an (approximate) complete result for $\rho'_v \to \gamma\gamma$ via the H^-H^+ loops we cannot simply add $T_H^{(1)}(k^2)$, (3.34), and $T_H^{(2)}(k^2)$, (3.19). This would imply a double counting of the threshold region. We shall thus subtract from $T_H^{(2)}(k^2)$ the contribution from the threshold region. From the properties of $T_H^{(2)}(k^2)$ we see that it satisfies an unsubtracted dispersion relation

$$T_H^{(2)}(k^2) = \frac{1}{\pi} \int_{4m_{H^\pm}^2}^\infty ds \, \frac{\text{Im}\left(T_H^{(2)}(s)\right)}{s - k^2 - i\epsilon} \tag{3.35}$$

with

$$\text{Im}\left(T_H^{(2)}(s)\right) = \frac{1}{2\pi} \frac{m_{\rho'}^2 + 2m_{H^\pm}^2}{v_0 m_{H^\pm}^2} \left(\frac{m_{H^\pm}^2}{s}\right)^2 \ln\left(\frac{1 + \sqrt{1 - 4m_{H^\pm}^2/s}}{1 - \sqrt{1 - 4m_{H^\pm}^2/s}}\right) \theta(s - 4m_{H^\pm}^2). \tag{3.36}$$

We choose now a function $\chi(s, E_0)$ defined for $s \geq 4m_{H^\pm}^2$ with the properties

$$\chi(4m_{H^\pm}^2, E_0) = 1, \quad \chi(s, E_0) = 0 \text{ for } s \gg 4m_{H^\pm}^2 + 4m_{H^\pm}E_0, \quad \chi(s, E_0) \text{ monotonously decreasing.} \tag{3.37}$$

With this function we set

$$\text{Im}\left(T_H^{(3)}(s)\right) = -\chi(s, E_0) \, \text{Im}\left(T_H^{(2)}(s)\right) \tag{3.38}$$

and

$$T_H^{(3)}(s) = \frac{1}{\pi} \int_{4m_{H^\pm}^2}^\infty ds \frac{\text{Im}(T_H^{(3)}(s))}{s - k^2 - i\epsilon}. \tag{3.39}$$

We set for the complete contribution of the $H^\pm$ loops to the function $T(k^2)$ in (3.14)

$$T_H(k^2) = T_H^{(1)}(k^2) + T_H^{(2)}(k^2) + T_H^{(3)}(k^2). \tag{3.40}$$

By construction $T_H^{(3)}(k^2)$ cancels out the threshold contribution of $T_H^{(2)}(k^2)$. In practical calculations we shall choose the function $\chi(s, E_0)$ (3.37) such that $\text{Im}\left(T_H(k^2)\right)$ has a smooth behaviour in the transition region from threshold to continuuum.

Putting everything together we have for the function $T(k^2)$ of (3.14) from (3.15), (3.18), and (3.40)

$$T(k^2) = \sum_{f=t,b,\tau} T_f(k^2) + T_W(k^2) + T_H(k^2). \tag{3.41}$$

The decay width of the virtual particle ρ'_v is then

$$\Gamma(\rho'_v(k^2) \to \gamma\gamma) = \frac{\pi}{4}\alpha^2 \left(k^2\right)^{3/2} |T(k^2)|^2. \tag{3.42}$$

.

4. DISCUSSION

Looking at the result (3.34) for $\rho'_v \to \gamma\gamma$ from the H^-H^+ loop in the threshold region we see that it corresponds to a superposition of resonance contributions. The positions of the resonances are approximately at $k^2 = 4m^2_{H^\pm}$, the widths are $2\Gamma_H$. Thus, the MCPM predicts such a type of resonance structure in the $\gamma\gamma$ spectrum. To give a concrete example we shall now choose the mass of $H^\pm$ to be

$$m_{H^\pm} = 375 \text{ GeV}. \tag{4.1}$$

Then, we get from section 3.1 of [10] that the main fermionic decays of $H^\pm$ are

$$H^- \to s\bar{c}, \qquad H^+ \to c\bar{s} \tag{4.2}$$

giving a decay rate (see table 3 of [10])

$$\Gamma(H^- \to s\bar{c}) = \Gamma(H^+ \to c\bar{s}) = 22.7 \text{ GeV}. \tag{4.3}$$

The decays

$$H^- \to h' + W^-, \quad H^+ \to h' + W^+, \quad H^- \to h'' + W^-, \quad H^+ \to h'' + W^+ \tag{4.4}$$

can occur in the MCPM if they are energetically possible. But, as we will argue below, even then their contribution to the total width of $H^\pm$ should be small. Thus, the best estimate for the total width of $H^\pm$ of mass (4.1) is

$$\Gamma_H \equiv \Gamma_{H^-} = \Gamma_{H^+} \approx 22.7 \text{ GeV}. \tag{4.5}$$

The branching fraction of $H^- \to \mu^-\bar{\nu}_\mu$ ($H^+ \to \mu^+\nu_\mu$) is then estimated to be (see (3.25) of [10])

$$\frac{\Gamma(H^- \to \mu^-\bar{\nu}_\mu)}{\Gamma_H} = \frac{\Gamma(H^+ \to \mu^+\nu_\mu)}{\Gamma_H} \approx 3 \times 10^{-5}. \tag{4.6}$$

With such a charged Higgs-boson pair $H^\pm$ and ρ' with masses given in (4.1) and (2.1), respectively, we get a rather strong attractive potential (3.21) with

$$\kappa = 0.21. \tag{4.7}$$

Thus, due to this potential, the MCPM predicts a resonance structure in the $\gamma\gamma$ channel at

$$2\, m_{H^\pm} = 750 \text{ GeV} \tag{4.8}$$

with a width

$$2\,\Gamma_H \approx 45.4 \text{ GeV}. \tag{4.9}$$

We note now that the ATLAS and CMS collaborations have indeed reported preliminary evidence for a sort of resonance structure at $m_{\gamma\gamma} \approx 750$ GeV with a width of the order of 45 GeV; see [19, 20]. Of course, we must be very careful and cannot yet identify the resonance structures discussed in section 3 of this paper with this possible experimental finding. In any case, we shall have to make a numerical study of the predicted effect. We shall do this in a separate paper. Here we shall only draw some conclusions based on the *hypothesis* that indeed the structure in the $\gamma\gamma$ spectrum at $m_{\gamma\gamma} = 750$ GeV is real and that it has something to do with the here discussed threshold effects.

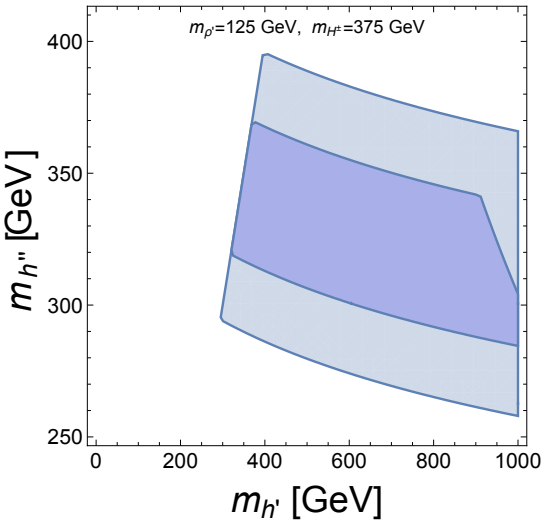

FIG. 7: The allowed regions for the masses of Higgs bosons h' and h'' in the MCPM given $m_{\rho'} = 125$ GeV, $m_{H^\pm} = 375$ GeV and the measured values of the oblique parameters S, T, U [21]. The dark and bright regions correspond to the 1σ and 2σ uncertainties, respectively.

The immediate consequence of the above hypothesis is that there should be a charged Higgs-boson pair $H^\pm$ at roughly $1/2 \times 750$ GeV $= 375$ GeV with the decay properties discussed in [10] and summarised in (4.2)-(4.6) here. We can also say something on the masses of the pseudoscalar (h'') and the scalar (h') Higgs bosons of the MCPM. For this we adapt the analysis of the oblique parameters S, T, U done in [13] for the case $m_{\rho'} = 125$ GeV, $m_{H^\pm} = 375$ GeV (see Fig. 2 of [13]). The resulting range for $m_{h''}$ versus $m_{h'}$ is shown in Fig. 7. We see that in the MCPM the masses $m_{h''}$ and $m_{h'}$ are predicted to be of the same order, if not higher, than $m_{H^\pm}$. Thus, the decays (4.3) should play no role for this mass constellation. The phenomenology of h'' and h' has been discussed extensively in [9–14]. We expect the main production modes to be of the Drell-Yan type

$$c\bar{c} \to h'', h' \quad \text{and} \quad s\bar{s} \to h'', h'. \tag{4.10}$$

The main decays are predicted to be (see Fig. 8 of [10])

$$h'' \to c + \bar{c}, \qquad h'' \to H^\pm + W^\mp \text{ if energetically possible,} \tag{4.11}$$

and

$$h' \to c + \bar{c}, \qquad h' \to H^\pm + W^\mp, h'' + Z \text{ if energetically possible.} \tag{4.12}$$

Here we have (see table 3 of [10])

$$\Gamma(h'' \to c\bar{c}) = 12.08 \text{ GeV} \left(\frac{m_{h'}}{200 \text{ GeV}}\right), \quad \Gamma(h' \to c\bar{c}) = 12.08 \text{ GeV} \left(\frac{m_{h''}}{200 \text{ GeV}}\right). \tag{4.13}$$

For the decay rates $h'' \to \mu^+\mu^-$ and $h' \to \mu^+\mu^-$ the prediction is (see (3.25) of [10])

$$\frac{\Gamma(h'' \to \mu^-\mu^+)}{\Gamma(h'' \to c\bar{c})} \approx 3 \times 10^{-5}, \quad \frac{\Gamma(h' \to \mu^-\mu^+)}{\Gamma(h' \to c\bar{c})} \approx 3 \times 10^{-5}. \tag{4.14}$$

5. CONCLUSIONS

In this article we have discussed the reaction $pp \to \gamma\gamma X$ in the MCPM. We found that this special two-Higgs-doublet model predicts a resonance type structure at $m_{\gamma\gamma} \approx 2m_{H^\pm}$ with a typical width $2\,\Gamma_H$. If this resonance structure in the $\gamma\gamma$ channel is tentatively put at 750 GeV we predict its width to be around 45.4 GeV. Furthermore, we predict $m_{H^\pm} \approx 375$ GeV and for the pseudoscalar (h'') a mass in the range 260 to 400 GeV and $m_{h'} > m_{h''}$. In addition, the MCPM makes definite predictions for the production and decay of the bosons $H^\pm$, h'', h' as discussed in [10–14]. A detailed numerical study of the above $\gamma\gamma$ resonance-like structure will be presented elsewhere.

Acknowledgments

The authors are grateful to W. Bernreuther for providing very useful information concerning the calculation of threshold effects. This work is supported partly by the Chilean research project FONDECYT with project number 1140568 as well as by the group of *Física de Altas Energias* of the UBB, Chile.

[1] G. Aad *et al.* [ATLAS Collaboration], "Observation of a new particle in the search for the Standard Model Higgs boson with the ATLAS detector at the LHC," Phys. Lett. B **716**, 1 (2012) [arXiv:1207.7214 [hep-ex]].

[2] S. Chatrchyan *et al.* [CMS Collaboration], "Observation of a new boson at a mass of 125 GeV with the CMS experiment at the LHC," Phys. Lett. B **716**, 30 (2012) [arXiv:1207.7235 [hep-ex]].

[3] J. F. Gunion, H. E. Haber, G. L. Kane and S. Dawson, "The Higgs Hunter's Guide," Front. Phys. **80**, 1 (2000).

[4] G. C. Branco, P. M. Ferreira, L. Lavoura, M. N. Rebelo, M. Sher and J. P. Silva, "Theory and phenomenology of two-Higgs-doublet models," Phys. Rept. **516**, 1 (2012) [arXiv:1106.0034 [hep-ph]].

[5] F. Nagel, "New aspects of gauge-boson couplings and the Higgs sector," PhD-thesis, Heidelberg University (2004), `http://www.ub.uni-heidelberg.de/archiv/4803`

[6] M. Maniatis, A. von Manteuffel, O. Nachtmann and F. Nagel, "Stability and symmetry breaking in the general two-Higgs-doublet model," Eur. Phys. J. C **48**, 805 (2006) [hep-ph/0605184].

[7] M. Maniatis, A. von Manteuffel and O. Nachtmann, "Determining the global minimum of Higgs potentials via Groebner bases: Applied to the NMSSM," Eur. Phys. J. C **49**, 1067 (2007) [hep-ph/0608314].

[8] M. Maniatis, A. von Manteuffel and O. Nachtmann, "CP violation in the general two-Higgs-doublet model: A Geometric view," Eur. Phys. J. C **57**, 719 (2008) [arXiv:0707.3344 [hep-ph]].

[9] M. Maniatis, A. von Manteuffel and O. Nachtmann, "A New type of CP symmetry, family replication and fermion mass hierarchies," Eur. Phys. J. C **57**, 739 (2008) [arXiv:0711.3760 [hep-ph]].

[10] M. Maniatis and O. Nachtmann, "On the phenomenology of a two-Higgs-doublet model with maximal CP symmetry at the LHC," JHEP **0905**, 028 (2009) [arXiv:0901.4341 [hep-ph]].

[11] M. Maniatis and O. Nachtmann, "On the phenomenology of a two-Higgs-doublet model with maximal CP symmetry at the LHC. II. Radiative effects," JHEP **1004**, 027 (2010) [arXiv:0912.2727 [hep-ph]].

[12] M. Maniatis, O. Nachtmann and A. von Manteuffel, "On the phenomenology of a two-Higgs-doublet model with maximal CP symmetry at the LHC: Synopsis and addendum," arXiv:1009.1869 [hep-ph].

[13] M. Maniatis and O. Nachtmann, "Symmetries and renormalisation in two-Higgs-doublet models," JHEP **1111**, 151 (2011) [arXiv:1106.1436 [hep-ph]].

[14] J. Brehmer, V. Lendermann, M. Maniatis, O. Nachtmann, H.-C. Schultz-Coulon and R. Stamen, "Towards testing a two-Higgs-doublet model with maximal CP symmetry at the LHC: construction of a Monte Carlo event generator," Eur. Phys. J. C **73**, no. 4, 2380 (2013) [arXiv:1209.2537 [hep-ph]].

[15] V. S. Fadin and V. A. Khoze, "Threshold Behavior of Heavy Top Production in e+ e- Collisions," JETP Lett. **46**, 525 (1987) [Pisma Zh. Eksp. Teor. Fiz. **46**, 417 (1987)].

[16] V. S. Fadin and V. A. Khoze, "Production of a pair of heavy quarks in e+ e- annihilation in the threshold region," Sov. J. Nucl. Phys. **48**, 309 (1988) [Yad. Fiz. **48**, 487 (1988)].

[17] V. S. Fadin, V. A. Khoze and T. Sjöstrand, "On the threshold behaviour of heavy top production," Z. Phys. C **48**, 613 (1990).

[18] M. J. Strassler and M. E. Peskin, "Threshold production of heavy top quarks: QCD and the Higgs boson," Phys. Rev. D **43**, 1500 (1991).

[19] The ATLAS collaboration, "Search for resonances in diphoton events with the ATLAS detector at $\sqrt{s} = 13$ TeV," ATLAS-CONF-2016-018, url: `https://cds.cern.ch/record/2141568`.

[20] CMS Collaboration, "Search for new physics in high mass diphoton events in 3.3 fb^{-1} of proton-proton collisions at $\sqrt{s} = 13$ TeV and combined interpretation of searches at 8 TeV and 13 TeV," CMS-PAS-EXO-16-018, url: `https://cds.cern.ch/record/2139899`.

[21] K. A. Olive *et al.* [Particle Data Group Collaboration], "Review of Particle Physics," Chin. Phys. C **38**, 090001 (2014).